

Pilot and full-scale validation of thickener and feedwell modelling

P.D. Fawell *Parker Centre (CSIRO Process Science and Engineering), Australia*

K. Simic *Parker Centre (CSIRO Process Science and Engineering), Australia*

K. Mohanarangam *Parker Centre (CSIRO Process Science and Engineering), Australia*

D.W. Stephens *Parker Centre (CSIRO Mathematical and Information Sciences), Australia*

M. Rudman *CSIRO Mathematical and Information Sciences, Australia*

D. Paterson *CSIRO Mathematical and Information Sciences, Australia*

W. Yang *CSIRO Process Science and Engineering, Australia*

J.B. Farrow *Parker Centre (CSIRO Process Science and Engineering), Australia*

Abstract

Advanced Computational Fluid Dynamics (CFD) modelling techniques are well suited for examining suspension flow patterns within feedwells and thickeners from which improved design options can be developed and evaluated. However, the confidence to rely upon recommendations based upon CFD requires model validation, something that is not readily achieved without a major commitment of resources. This paper outlines a number of experimental validation procedures applied to test CFD models for different thickening zones as part of the AMIRA P266 “Improving Thickener Technology” series of projects.

1 Introduction

As the power and speed of computational fluid dynamics (CFD) techniques increases, the attractiveness of applying these models to industrial processes also rises, largely due to being much faster and much more cost-efficient than most experiments, particularly when focused on full-scale issues.

However, it is the commitment to validation that differentiates the serious researchers from dabblers with access to software. Anderson and Papachristodoulou (2009) state that “In principle the only statement that one can make about a system model is that it is incorrect, i.e., invalid, a fact which can be established given appropriate experimental data.” It is rare that small-scale validation measurements alone, in which vessel dimensions are highly constrained, can provide confidence that CFD models can be extended to capture real behaviour in three dimensions. Substantial validation is required at either pilot or full-scale, although the number of such measurements that can be conducted will inevitably be limited by time and resources. While complete validation is therefore a practical impossibility, effective invalidation of interim models can be achieved and represents an important step in viable model development.

The AMIRA P266 “Improving Thickener Technology” series of projects has been applying CFD modelling to the study of gravity thickening in mineral processing since 1993 (Kahane et al., 2002; Nguyen et al., 2006; Fawell et al., 2009). The commercial CFD code was initially limited to the prediction of fluid velocity, solids distribution and shear rates, although even that required considerable expertise in developing specific models to describe feedwell processes, such as deciding upon the most appropriate description for turbulence. Even so, the early P266 applications were similar to the approach being taken by others using CFD to minimise currents in water treatment clarifiers. However, significant advances were made once the P266 models were customised to incorporate the flocculation process, first giving predictions of flocculant adsorption and then of aggregate size throughout a feedwell. Further advances included separate CFD models for the prediction of torque and slurry transport from rakes. The most recent advances include the incorporation of bed properties and the effects of shear on dewatering of compressible flocculated suspensions, as well as linking various sub-models towards the goal of full thickener modelling. While feedwell optimisation from CFD has by itself been successful in improving thickener underflow density, full thickener modelling is expected to be an ever more powerful tool for achieving desirable underflow properties.

A thickener can be broken up into four regions for validation studies:

- Feedwell (intermediate solids, high velocity).
- Clarification zone (low solids, low velocity).
- Settling zone (intermediate solids, intermediate velocities).
- Rake zone (high solids, low velocity).

A CFD model can be used to generate a velocity flow field as a primary output, but can also predict a residence time distribution (RTD) for the addition of a tracer in a nominated location as a secondary output. Clearly measurements of the primary output are preferred, but have not (until recently) been practical to achieve across the spectrum of conditions encountered in the four zones described above.

This paper provides a brief description of solid and liquid tracers used to measure RTDs for the processes observed in the different thickener zones and how they have either given confidence in the use of the corresponding CFD models or been used to improve them. The evolution of velocity measurements will also be outlined, focusing on the new ultrasonic velocity profiling technique that offers rapid mapping capabilities, potentially across a range of solids concentrations. Validation of other thickener performance measures will also be briefly discussed.

2 Liquid tracer

Effective CFD model validation requires many repeat tracer runs to obtain an average suitable for comparing with the CFD predictions. Stable operating conditions are therefore required; on the full-scale this is more easily achieved within the feedwell than the whole thickener.

Early efforts within P266 to achieve validation of flow field predictions focused on liquid phase tracers, in which a tracer element was added to the feed or feedwell, with samples taken at nominated positions at known times. The tracer element must be distinguishable from species present in the process liquors, and their selection governed by analysis techniques available at the operating site (generally atomic absorption spectroscopy). Such elements must exhibit stability in the process liquor, be cost-effective and be easily handled (safe to use, readily solubilised within an appropriate liquor and at concentrations that allow rapid injection). Table 1 lists elements that have been successfully used in various applications.

Table 1 Tracers applied during P266 projects in feedwell and thickener flow structure validation

Tracer Element	Solid Form	Application
Li ⁺	LiOH.H ₂ O	Bauxite residue
Na ⁺	NaCl	Mineral sands tailings
Na ⁺	Na ₂ SO ₄	Zinc processing (acidic solutions)
K ⁺	KOH	Coal tailings
Li ⁺	LiCl	Zinc processing (acidic solutions)

The general requirement upon which the tracer experiments are designed is to achieve a tracer element concentration of 40 mg L⁻¹ averaged across the vessel volume (be that the feedwell or the full thickener). Tracers were prepared in overflow liquor and the injected volumes have varied from 13 L to 3 m³. Lower make-up volumes are preferred, but low solubility of the element's salt in the liquor can lead to volumes at the higher end of the range. After tracer addition, grab samples are taken at particular times, although it is preferable to use a multi-head pump to simultaneously remove slurry/liquor from tubes at the selected sampling locations.

An example of the use of a liquid tracer in CFD validation is provided in Figure 1 for the feedwell of a thickener used in the processing of zinc concentrates. The left image shows the CFD prediction of the velocity vectors within the feedwell. This was one of the earliest applications of CFD during P266, in which the slurry was modelled as a single phase. On this basis, CFD predicts the closed feedwell is well mixed, and

that the discharge from the base of the feedwell is symmetrical (residence time plots, bottom right). However, the tracer profiles for the four sampling positions (top right) clearly show asymmetrical discharge.

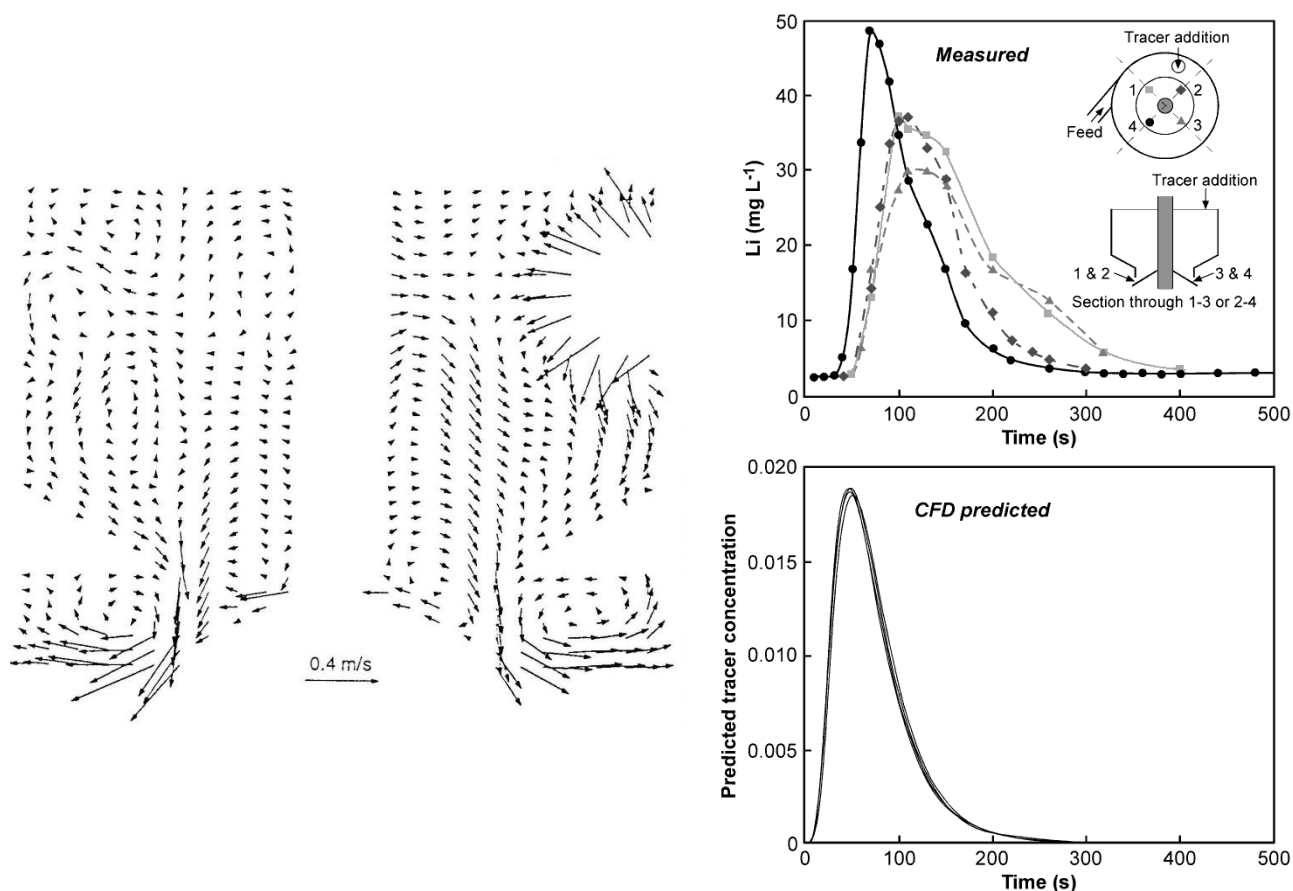


Figure 1 Single-phase CFD velocity field prediction of velocity vectors within the feedwell of a thickener from a zinc plant (left); measured and CFD predicted profiles for Li⁺ tracer added to the feedwell (right)

The use of a single phase modelling approach may have some value in the study of low solids/low particle density systems such as those encountered in wastewater treatment feedwells, but Figure 1 served to invalidate this approach for feedwell studies in mineral processing applications. Higher solids streams entering a feedwell can sink appreciably before being dispersed, greatly influencing overall flow patterns. All subsequent feedwell CFD modelling through the P266 projects utilised a multi-phase approach, and this has led to much better agreement between measured and modelled tracer profiles.

CFD is frequently used to model clarification zones within wastewater treatment vessels that typically have very low rise velocities, and therefore any currents can readily entrain slow settling solids to the overflow (e.g. Brouckaert and Buckley, 1999; Laine et al., 1999). The same approach can have relevance to the study of clarifiers within mineral processing, and this was tested experimentally in P266 through sodium tracer addition to a clarifier operating at $\sim 75^{\circ}\text{C}$. Details of the tracer procedures have been published previously (Johnston et al., 1998).

The left image in Figure 2 shows the six overflow sampling positions on a plan view of the clarifier, with the tracer profiles split into two distinct groups on the right. The tracer profiles were inconsistent with initial CFD modelling; while an asymmetric feedwell discharge was predicted, this did not match with the observed pattern. However, this modelling assumed there was no thermal gradient within the unit, whereas subsequent temperature measurements showed an increase in temperature with depth of $\sim 0.2^{\circ}\text{C m}^{-1}$. Thermal convection was likely to result from heat losses through walls and the free surface, and this can create a toroidal vortex flow pattern. Spot velocities (discussed in Section 3) were measured at 0.5 m intervals from the free surface

to just above the rake, and were used to successfully test a CFD model that took into account thermal convection. With thermal effects considered, CFD better predicted the tracer profiles.

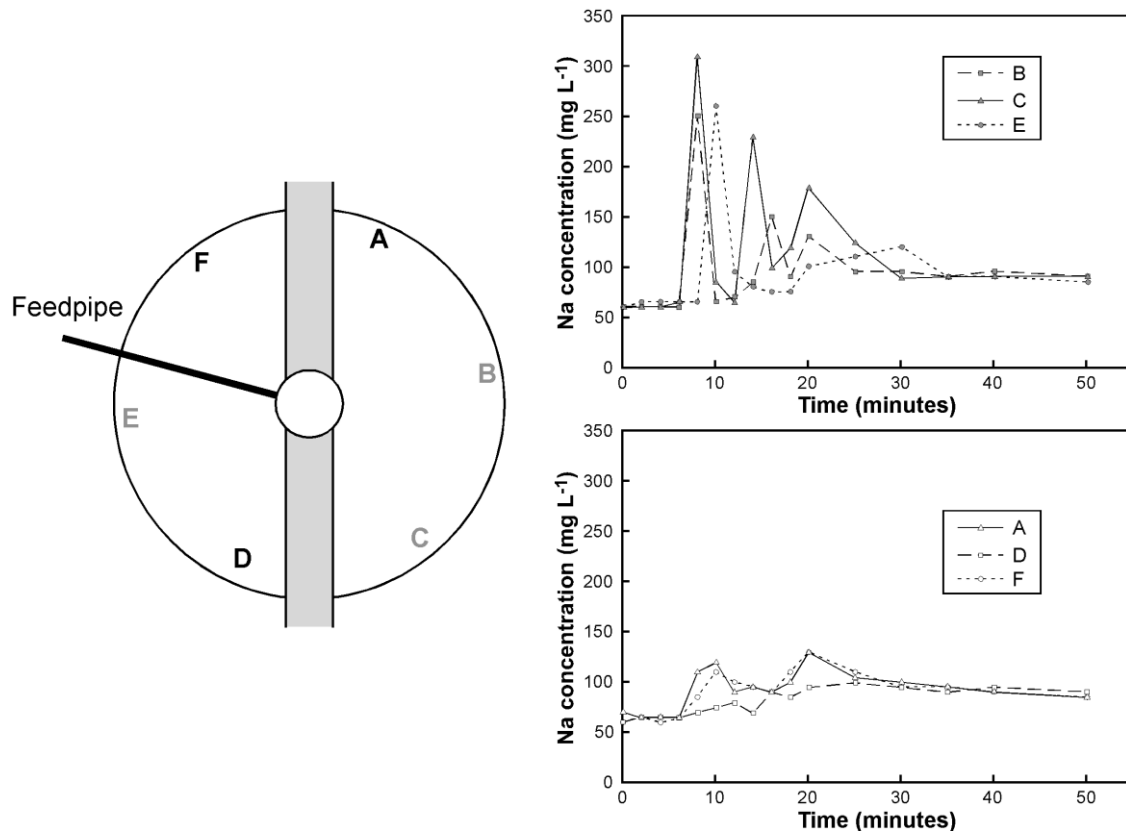


Figure 2 Overflow sampling points following Na^+ tracer addition to the feedwell of a clarifier from a zinc plant (left); measured tracer profiles from the different sampling points (right)

Tracer sampling suffers from several short-comings, most of which relate to analysis. The number of runs that can be achieved is generally limited by the site's laboratory capacity for additional throughput; in practice, two runs a day is normally a maximum, and two runs \times four sampling points \times >20 sample times at each point represents at least 180 samples for analysis. Regardless of the laboratory's efficiency, the results are not obtained in real-time and feedback on the tests can be delayed. It may not be practical to increase sampling frequency, and as a consequence, peak detection can be difficult. There would be clear advantages to having a real-time analytical technique that can be applied across a whole thickener.

The use of specific ion electrodes for on-line analysis has been tested at a pilot thickener scale. They offer real time, continuous concentration data, and therefore feedback is essentially immediate. It is therefore possible and much more practical to conduct numerous runs to obtain time average tracer response curves for direct comparison with CFD model prediction. Tests with a 1 m diameter pilot tank and nitrate-selective electrodes at selected overflow positions allowed the averaging of over 20 runs, with peak positions very well captured. With electrodes in fixed locations, concerns over the impact of sampling on hydrodynamics are eliminated. As yet, such electrodes have not been applied on full scale thickeners within the P266 projects.

3 Velocity measurements

The velocity measurements mentioned above highlighted the danger of relying upon spot velocities measured in only one or a few locations, since density currents can develop in clarification zones with low rise velocities that can affect overflow performance, but may not be readily detected by measurements limited to the surface layers. The acquisition of 2D measurements in a vertical plane is therefore desirable.

Early measurements were made with an electromagnetic velocity meter (Sensa-RS3). This provided single point intrusive velocity measurements in the range $\pm 10 \text{ m s}^{-1}$, requiring a conductive liquid phase. The sampling rate was slow (2 Hz) and generating even basic 2D information (lowering to different heights and then moving to the next available location) was a time-consuming process.

This was improved upon with the use of acoustic Doppler velocimetry (ADV). The Sontek ADV probe has three arms that act as acoustic receivers to the signal transmitted from the centre of the arms, the received signal then processed into x, y and z coordinates of the flow in units of cm s^{-1} . The probe is less intrusive, and while the presence of particles is essential for the measurement, the required level is generally achieved within thickeners without additional seeding. However, this was still only a single point measurement.

An ultrasonic velocity profiler (UVP) is available that has the potential to provide profiles in most zones within a thickener. A single UVP probe is a transceiver that emits an ultrasound signal and then receives the echoes off reflected particles in the beam, with the received signal processed to generate velocities at known distances from the probe (up to 3 m). A single probe can provide a velocity profile in pipe flow, whereas multiple probes can generate a 2D flow field (Figure 3). The Met-Flow UVP-Duo can potentially be linked to 20 probes in one measurement configuration; again, the presence of particles is required, but only at very low levels. UVP also offers much higher sampling rates than electromagnetic measurements (up to 100 Hz) and has greater sensitivity to low velocities.

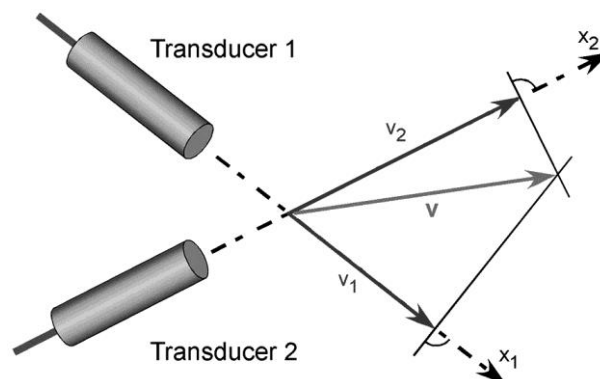


Figure 3 Schematic representation of 2D flow field generation by multiple UVP probes (adapted from Met-Flow UVP-Duo user manual)

The direct relevance of UVP to flow characterisation in the clarification zone is readily apparent and relatively straightforward. However, the measurement of flow structures that result from multiphase flows in a feedwell (critical for validation of CFD model predictions) is a more challenging application of the UVP system. As a first step, an open feedwell with shelf and tangential feed was used to examine the feasibility of the technique.

A 600 mm diameter pilot-scale feedwell was mounted in a 5 m^3 water tank, with water pumped out of the side of the tank base and recirculated back through the feedwell. The water was seeded with calcite (Omyacarb 2) particles. The solids content was less than 0.1% w/w, which for this purpose was considered insignificant, so that single phase flow was assumed. However, it should be noted that the fluid was still opaque enough to render other available velocity techniques inappropriate.

UVP transducers were mounted within the plastic rake shaft and on a bar at the free surface to provide the necessary configuration to map the flow structure. The selected resolution in the vertical and horizontal positioning of the transducers was 25 and 20 mm, respectively. At each transducer position, 500 velocity profiles were taken to obtain a time-averaged velocity profile along the direction of the transducer beam. The orthogonal intersection of the ultrasound beams allows the resultant velocity vector to be determined at the desired point in space (Figure 3), hence with multiple intersections, the flow structure may be determined experimentally.

Figure 4 shows the measured time-averaged flow structure through one half of section AA in the feedwell. The positions of the shelf and feed pipe are denoted in red on the flow field. The feed flow (nominally 1.5 m s^{-1} in the 50 mm feedpipe) is out of the page and clockwise through the feedwell.

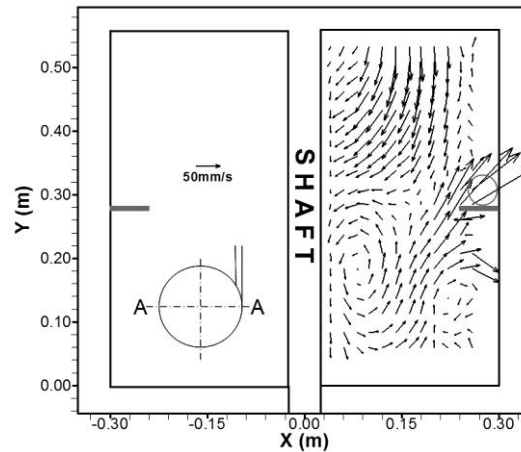


Figure 4 Measured vertical flow field through half of section AA. Insert shows the measurement plane with respect to feedpipe entry. Shelf size $D/10$ and feed inlet velocity 1.5 m s^{-1}

Above the feed inlet, flow is directed inwards and downwards toward the rake shaft due to the incoming feed. This becomes horizontal at the level of the feedpipe, before being directed downward by the rake shaft. The presence of recirculation zones below the shelf is evident, indicating that the flow structure is complex. The measured features in the flow are similar to those observed in small-scale laser-based measurements (e.g. White et al., 2003) that are also limited to very low solids concentrations.

This data is the first obtained with the UVP technique for thickener feedwells. Although preliminary, the results are very encouraging, with a high prospect of using UVP to map the multiphase flow structure in detail. More recent work has fine-tuned the measurement procedure and developed appropriate data analysis and interpretation protocols. Vertical flow structures as well as detailed flow structures at selected horizontal planes (e.g. feedwell discharge) are being measured.

Also of great interest is the potential to use UVP to quantify unsteady or transient flow behaviour. Although not presented here, some flow unsteadiness was observed in the data set used to develop the flow structure in Figure 4. Such information would be invaluable in understanding the operation of some thickener feedwell designs. Unsteady behaviour has been observed experimentally in tomographic imaging studies of feedwells, but tomography in this application does not offer reliable quantification. In some CFD studies the models were not able to converge to a steady-state solution due to the transient flows generated by such feedwells. The effect that transient behaviour has on flocculation is not known at this stage.

4 Solids tracer in raking studies

Rakes in conventional units are used to assist the transport of the sediment bed to the underflow and to aid dewatering through the shearing action generated by the rake. Sediment transport in a thickener is the combination of mechanical transport by the rakes and gravitational effects. The sediment rheology has an important influence on rake torque and on efficient sediment transport due to gravity, but not much influence on the rate of transport by raking. Other factors such as rake speed and rake design have less influence on torque but do, however, have a critical bearing on the efficient transport of the sediment bed to the underflow. As a result of CFD modelling undertaken in P266, the effects of changes in rake design on rake torque, sediment transport and the degree of shear imparted on the sediment can now be estimated and conditions for satisfactory rake operation can be identified. Rake torque models of varying sophistication are well known and as their validation is relatively straight-forward, they will not be discussed further. In contrast, validation of 3D shear predictions within a raked bed is currently not viable. The discussion below therefore focuses on sediment transport effects.

The pilot-scale thickener facility used in this study is a closed loop system and is shown schematically in Figure 5 (for full details, see Rudman et al., 2008). A sample of slurry is mixed continuously in a 4.5 m^3 mixing tank and then pumped into the pilot thickener. The thickener is a 2 m diameter by 2 m high sidewall tank with a 14° floor and a small discharge hopper (45° slope). This “thickener” is not used as a

sedimentation and dewatering tank in the experiments reported here; instead it plays the role of a through-flow holding tank in which the raking experiments are undertaken. The slurry is distributed into the thickener uniformly across a radius via a ring manifold. Underflow from the pilot thickener is fed back into the mixing tank. An on-board Proportional-Integral-Derivative (PID) program in the variable frequency drive uses a feedback signal from the ultrasonic level sensor to maintain a stable slurry height. Underflow was regulated by a PID loop and flow meter combination. Other variables monitored on the underflow include density and temperature.

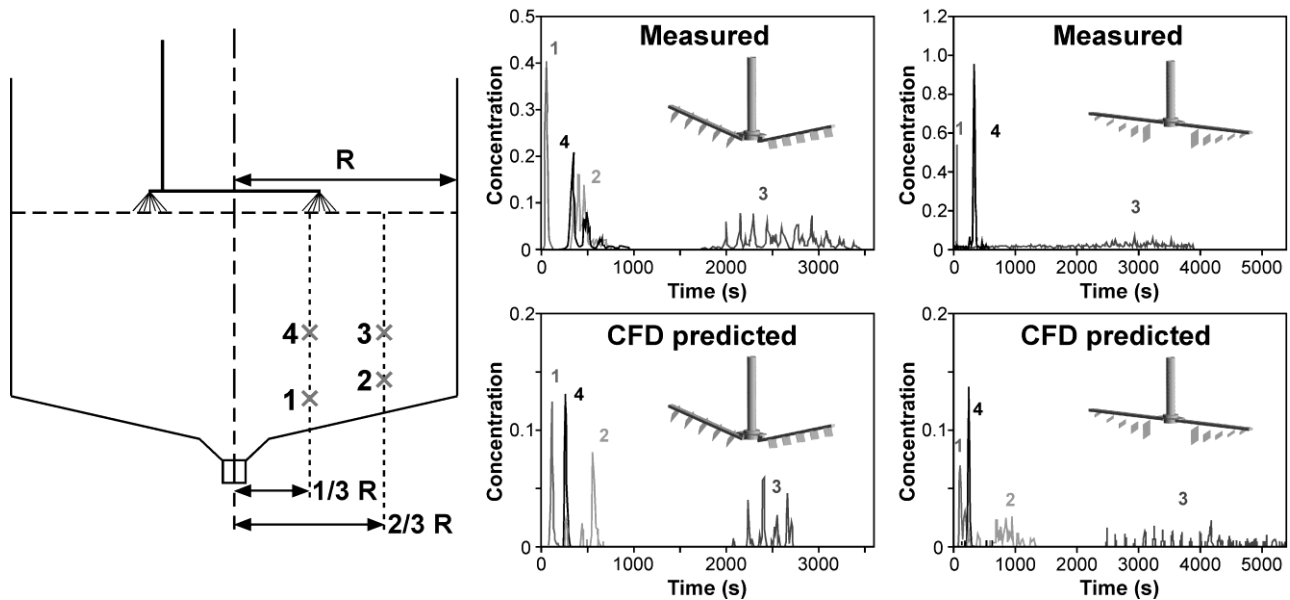


Figure 5 Measured and CFD predicted profiles for solid tracer (dyed kaolin) added at four different locations to a clay bed raked with constant and variable height blades at 0.2 rpm

Once steady slurry height and underflow conditions were attained in the thickener tank, the rake was turned on. The rake is mounted on a central shaft that was driven by a motor and gearbox at speeds between 0.2 and 2 rpm. The tip speed of the outer blade at 1 rpm corresponds to the same tip speed as that in a 40 m thickener operating at a rake speed of 3 rev h⁻¹. A variable frequency drive was used to control the rake speed either by manual setting or by utilising the on-board programming capabilities.

The study was undertaken at a sand mining operation, with the clay-based feed (all sub 100 μm) being drawn from the underflow of the plant tailings thickener. X-ray diffraction analysis revealed that the feed solids contained a significant proportion of kaolinite that is known to strongly adsorb a range of commercially available dyes. Consequently, an optical technique was chosen to measure solids residence time distributions using a reflectance spectrometer. The dye Azure A was chosen because its colour response was more intense than alternatives. A saturated solids tracer slurry was prepared by mixing 2 g of Azure A with 1 kg of feed slurry (solids content 11.3 wt%) for 10 minutes. Dyed material was rheologically indistinguishable from undyed material and provided sufficient contrast at low concentrations for good detection.

Experiments were conducted with the 2 m pilot scale thickener fitted with either constant or variable height rake blades. For the latter, the height varies non-linearly (more rapidly near the centre), based on model predictions to ensure a more even inwards delivery of material from one blade to the next. To modify the rheology of the plant underflow, attapulgite clay was added and mixed until homogeneous. Slurry yield stresses of 3.2, 38 and 90 Pa were examined.

Tracer was released at four bed locations, as indicated by the left-hand schematic in Figure 5. This figure also shows that for both rake configurations at a rotation rate of 0.2 rpm with a yield stress of 38 Pa the tracer exits in the sequence 1, 4, 2 and 3. Tracer released at position 4 clearly preceding that from positions 2 and 3 indicates that the rake is not delivering much sediment to the underflow, with the underflow pumping and gravitational draining effects leading to short-circuiting to the underflow. Such short-circuiting is eliminated at higher rotation rates through increased rake delivery, and at 2 rpm the exit sequence changes to 1, 2, 3, 4

for the constant height rake. For the variable height configuration the tracer added at positions 3 and 4 exit at similar times, but clearly after 2. Identical tracer exit sequences were also observed for the 3.2 and 90 Pa yield stress slurries when comparisons were made at the same rake rotation rate, suggesting flow structures were fairly independent of the sediment bed rheology, but strongly dependent on rake speed.

Figure 5 shows a very good agreement between measured and CFD-predicted tracer responses, which was reflected for all conditions studied. This agreement provides some model validation, increasing the level of confidence that the model can be used to accurately predict sediment flow structures for different full-scale thickener rake designs and operating conditions. The potential of this capability is demonstrated in Figure 6, which presents CFD predicted full residence time contours in a vertical plane of the pilot thickener for the two rakes studied. The residence time distribution was broad at 0.2 rpm, with times of less than 1,000 s predicted near the centre (above the underflow), extending to over 6,000 s at the walls and near the outer blades. There were no major differences between the two rake configurations. In contrast, the increased inwards delivery at 2 rpm ensures that very long residence times near the walls and short-circuiting at the centre are virtually eliminated. The variable height rake produces a more uniform downflow, as evidenced by the more horizontal contours. Ideally, perfectly horizontal contours would be seen across the plane of the thickener. The experimental tracer sequence observed for the constant height blade configuration at 2 rpm, with tracer at position 4 leaving last, is indicative of recirculation outwards from over-delivery by the outer blades, and this has been supported by CFD velocity vector predictions (Rudman et al., 2008).

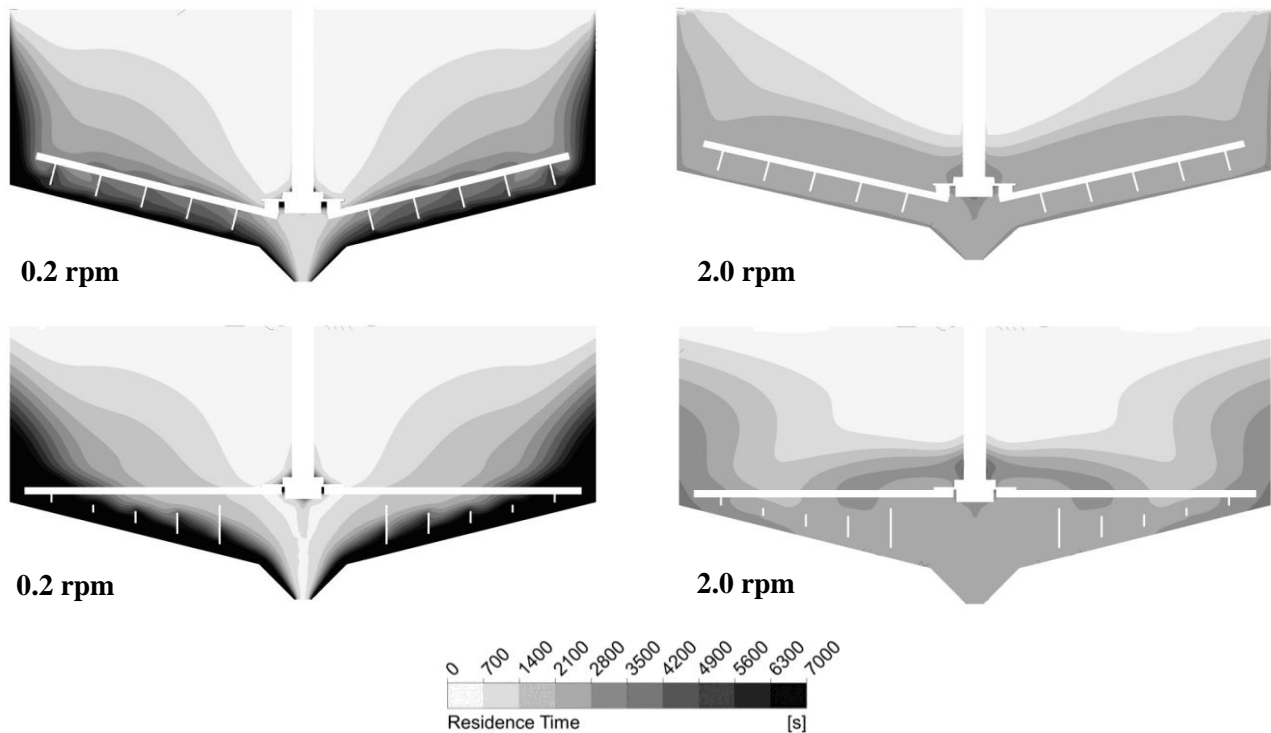


Figure 6 Contours of residence time on a plane through the rake for constant and variable height blade rakes (for rake speeds of 0.2 and 2 rpm) in a 2 m pilot thickener

The intention is to combine such information with predictions of shear rates and models for both sedimentation and aggregate dewatering to give the first predictions of underflow density that consider the contributions from raking. Towards this, it is necessary to extend the residence time studies to flocculated sediments. Recent work has identified tracer dyes that can be applied to clay slurries that do not impact significantly upon flocculation kinetics and the resultant aggregate properties.

5 Validation of other thickener performance measures

CFD can predict (or has the potential to predict) a number of other performance measures of relevance to gravity thickening. Some of these can readily be validated using currently available control instrumentation (e.g. overflow and underflow solids concentrations, bed height, bed solids profile). Others are more complicated, with the capacity for validation at varying degrees of development; these are discussed briefly below.

5.1 Residual flocculant

The CFD feedwell model developed through P266 is able to predict the distribution and adsorption of flocculant after dosing throughout a feedwell, with the estimated percentage of unabsorbed flocculant discharged at the exit plane often used as an indication of mixing efficiency (Kahane et al., 2002; Owen et al., 2009). Validation of this particular aspect of the model has not been achieved, other than indirectly from the repeated successful application to optimising feedwell design and sparge location in full-scale thickeners. While the model predictions of unabsorbed flocculant may exceed reality, the relative values for different operational configurations are still considered indicative of performance.

The difficulty of validating flocculant predictions reflects the very low concentrations that may be discharged even under poor feedwell mixing conditions, typically <1 ppm (Owen et al., 2008). An array of techniques exist for the quantification of acrylamide/acrylate copolymer solutions (e.g. Taylor and Nasr-El-Din, 1994), but none offer the sensitivity required in real process liquors within practical time-scales. The introduction of tracer functionalities (e.g. allowing fluorescence detection) has been highly successful with cationic flocculants used in wastewater treatment (Becker et al., 2004), allowing in-stream detection at very low levels. While such functionalities have been introduced into acrylamide/acrylate copolymers, they are not available at the high molecular weights used in mineral processing. Where such functionalities include bulky fluorescent groups, their impact on flocculant adsorption, flocculation kinetics and aggregate structures may also be of considerable concern. Practical quantification across a range of conditions is still best done by activity measurements (i.e. settling rate calibration from mixing supernatant with an appropriate standard slurry). It should also be noted that in most cases, actual detection of residual flocculant is itself sufficient to identify feedwell performance issues.

Paste-related applications are now known where very high flocculant dosages are applied, primarily to suspensions already at high solids concentrations. In such cases there may be a greater prospect of observing readily measurable residual flocculant concentrations, in particular from samples at shorter reaction times.

5.2 Aggregate size

Recent CFD modelling in P266 has provided aggregate size predictions through inclusion of a population balance model of flocculation kinetics (Nguyen et al., 2006). Aggregate size is often inferred from settling rate measurements obtained from feedwell sampling (i.e. in commercial instruments used with thickener control), although settling rates can be unreliable in this context without knowledge of the solids concentration. The most successful tool for real-time characterisation of aggregates has been focused beam reflectance measurement (FBRM), which involves collation of chord length reflections from particles and aggregates of a scanning laser beam focused at the slurry interface with the probe's sapphire window (Owen et al., 2008). This is used extensively in P266 to monitor flocculation in turbulent pipe flow, and to a lesser degree in feedwell studies, with the probe either inserted through the side of a pilot tank into the feedwell's exit plane, or submersed within a full-scale thickener. Similar submersion of an FBRM probe has been applied in wastewater thickeners (De Clercq et al., 2004). Analysis is complicated by the non-linear response of FBRM to solids concentration, while prior knowledge of the vessel hydrodynamics is critical to ensure correct presentation to the probe. Use of FBRM in such studies has been limited by the high cost of the probes.

Bizi and Gaboriau (2008) have applied laser diffraction (Malvern Mastersizer S) to obtain aggregate size distributions during the thickening of clay slimes from a quarry (feed solids $\sim 17 \text{ kg m}^{-3}$). Samples were gravity fed into a 10 mm measurement cell after external solids dilution under low shear to below the instrument's required obscuration limit (16%). This eliminated the need for sample recirculation and (they claim) reduced aggregate breakage, although the potential for further aggregate growth was not considered.

This approach may be difficult to adapt for control purposes, but the authors did note greater sensitivity to process changes than were observed from settling test measurements.

5.3 Feedwell solids

As discussed in Section 2, liquid tracers can be used in feedwell validation studies to indicate fluid flow, but it cannot always be assumed that this represents the path taken by solids. Feedwell sampling has been used to indicate solids loadings in various feedwell locations; at the pilot-scale, electrical resistance tomography has shown some promise, but requires more development. In terms of the solids discharged from feedwells and their subsequent sedimentation, iron powders have been applied under Bayer conditions (Leclerc et al., 2005), although it is questionable whether such particles can be assumed to mimic the behaviour of aggregates. It is possible that the dyed solids discussed at the end of Section 4 may also be an option in this respect, offering the potential to be incorporated in flocculated aggregates without altering the process. However, this would require substantial further development, and would at best have limited application beyond pilot studies with standard non-coloured clay slurries.

6 Conclusions

CFD modelling offers enormous potential for the optimisation of thickener design, and with the high performance requirements expected of paste thickeners, the application of CFD to new and existing units will only increase. The focus to date has been on feedwell performance, which by itself can have a major impact on underflow properties, but the successful integration of aggregate dewatering achieved within raked beds into sedimentation modelling would almost certainly provide a step change in the understanding of how to produce desirable paste properties.

The main risk comes from the use of CFD without at least some degree of model validation, as such validation is required to provide confidence that the physical and chemical processes are being adequately captured within the CFD predictions. For feedwell performance validation, this can be achieved through liquid tracer and velocity measurements. The latter, as a primary CFD output, is to be preferred and the UVP instruments now available make such measurements far more practical. Critically, the use of UVP may allow a greater range of operational conditions to be examined. Successful validation over more conditions gives much greater weight to the general applicability of the CFD model to the particular application, but even invalidation can either identify boundary conditions within which the model should be restricted or produce the experimental basis for further model refinement.

The validation of sedimentation and raking models (apart from the comparatively trivial comparison of underflow solids concentrations) is much more difficult. UVP may still be applicable at higher solids and much lower velocities to monitor fluid flows, but this is yet to be tested. Another major challenge is to demonstrate that solids tracers can be used successfully in flocculated systems without altering flocculation kinetics or aggregate structures.

Acknowledgements

The authors thank the sponsors of the AMIRA P266 'Improving Thickener Technology' series of projects for their financial and in-kind support.

This research has also received support from the Australian Government's Cooperative Research Centre (CRC) program, through the A.J. Parker CRC for Integrated Hydrometallurgy Solutions (the Parker Centre), as well as from CSIRO's Minerals Down Under National Research Flagship.

The direct involvement and contributions from numerous industry personnel has been crucial to the success of this work. The authors also wish to acknowledge the contributions from a wide range of CSIRO staff.

References

- Anderson, J. and Papachristodoulou, A. (2009) On validation and invalidation of biological models, *BMC Bioinformatics*, Vol. 10, p. 132.

- Becker, N.S.C., Bennett, D.M., Bolto, B.A., Dixon, D.R., Eldridge, R.J., Le, N.P. and Rye, C.S. (2004) Detection of polyelectrolytes at trace levels in water by fluorescent tagging, *Reactive and Functional Polymers*, Vol. 60, pp. 183–193.
- Bizi, M. and Gaboriau, H. (2008) Flocculation analysis and control system by laser diffractometry at industrial scale, *AIChE Journal*, Vol. 54, pp. 132–137.
- Brouckaert, C.J. and Buckley, C.A. (1999) The use of computational fluid dynamics for improving the design and operation of water and wastewater treatment plants, *Water Science and Technology*, Vol. 40(4-5), pp. 81–89.
- De Clercq, B., Lant, P.A. and Vanrolleghem, P.A. (2004) Focused beam reflectance technique for in situ particle sizing in wastewater treatment settling tanks, *Journal of Chemical Technology and Biotechnology*, Vol. 79, pp. 610–618.
- Fawell, P.D., Farrow, J.B., Heath, A.R., Nguyen, T.V., Owen, A.T., Paterson, D., Rudman, M., Scales, P.J., Simic, K., Stephens, D.W., Swift, J.D. and Usher, S.P. (2009) 20 years of AMIRA P266 ‘Improving Thickener Technology’ - how has it changed the understanding of thickener performance?, in *Proceedings 12th International Seminar on Paste and Thickened Tailings (Paste09)*, R.J. Jewell, A.B. Fourie, S. Barrera, J. Wiertz (eds), 21–24 April 2009, Viña Del Mar, Chile, Gecamin Limited, Santiago, Australian Centre for Geomechanics, Perth, pp. 59–68.
- Johnston, R.R.M., Schwarz, P., Newman, M., Kershaw, M., Farrow, J.B., Simic, K. and Swift, J.D. (1998) Improving thickener performance at Pasmenco Hobart Smelter, Zinc and Lead Processing, J.E. Dutrizac, J.A. Gonzalez, G.L. Bolton, P. Hancock (eds), *Canadian Institute of Mining, Metallurgy and Petroleum*, pp. 697–713.
- Kahane, R.B., Schwarz, M.P. and Johnston, R.R.M. (2002) Residue thickener modelling at Worsley Alumina, *Applied Mathematical Modelling*, Vol. 26, pp. 281–296.
- Laine, S., Phan, L., Pellarin, P. and Robert, P. (1999) Operating diagnostics on a flocculator-settling tank using Fluent CFD software, *Water Science and Technology*, Vol. 39(4), pp. 155–162.
- Leclerc, A., Boivin, A., Simard, G., Morin, L., Gagnon, M.J., Verreault, R. and Peloquin, G. (2005) Electromagnetic detection of iron tracers for monitoring particles displacement in gravity settlers, in *Proceedings Seventh International Alumina Quality Workshop*, Perth, Australia, 16–21 October, pp. 127–139.
- Nguyen, T., Heath, A. and Witt, P. (2006) Population balance – CFD modelling of fluid flow, solids distribution and flocculation in thickener feedwells, in *Proceedings Fifth International Conference on CFD in the Process Industries*, Melbourne, Australia, December 2006.
- Owen, A.T., Fawell, P.D., Swift, J.D., Labbett, D.M., Benn, F.A. and Farrow, J.B. (2008) Using turbulent pipe flow to study the factors affecting polymer-bridging flocculation of mineral systems, *International Journal of Mineral Processing*, Vol. 87, pp. 90–99.
- Owen, A.T., Nguyen, T.V. and Fawell, P.D. (2009) The effect of flocculant solution transport and addition conditions on feedwell performance in gravity thickeners, *International Journal of Mineral Processing*, Vol. 93, pp. 115–127.
- Rudman, M., Simic, K., Paterson, D.A., Strode, P., Brent, A. and Šutalo, I.D. (2008) Raking in gravity thickeners, *International Journal of Mineral Processing*, Vol. 86, pp. 114–130.
- Taylor, K.C. and Nasr-El-Din, H.A. (1994) Acrylamide copolymers: a review of methods for the determination of concentration and degree of hydrolysis, *Journal of Petroleum Science and Engineering*, Vol. 12, pp. 9–23.
- White, R.B., Šutalo, I.D. and Nguyen, T. (2003) Fluid flow in thickener feedwell models, *Minerals Engineering*, Vol. 16, pp. 145–150.

